Control of the multimillennial wildfire size in boreal North America by spring climatic conditions

Adam A. Ali[a,b,1,2], Olivier Blarquez[b,c,1], Martin P. Girardin[d], Christelle Hély[a,e], Fabien Tinquaut[f], Ahmed El Guellab[b,c], Verushka Valsecchi[a,e], Aurélie Terrier[c], Laurent Bremond[a,e], Aurélie Genries[b,c], Sylvie Gauthier[d], and Yves Bergeron[b,c]

[a]Centre de Bio-Archéologie et d'Ecologie, Unité Mixte de Recherche (UMR) 5059 Centre National de la Recherche Scientifique (CNRS), Université Montpellier 2, Institut de Botanique, F-34090 Montpellier, France; [b]Natural Sciences and Engineering Research Council of Canada Industrial Chair in Sustainable Forest Management, Forest Research Institute, Université du Québec en Abitibi-Témiscamingue, Rouyn-Noranda, QC, J9X 5E4 Canada; [c]Centre d'Etude de la Forêt, Université du Québec à Montréal, Montreal, QC, H3C 3P8 Canada; [d]Ressources Naturelles Canada, Service Canadien des Forêts, Centre de Foresterie des Laurentides, Québec, QC, G1V 4C7 Canada; [e]Paléoenvironnements et Chronoécologie (PALECO), École Pratique des Hautes Études (EPHE), Institut de Botanique, F-34090 Montpellier, France; and [f]Centre Européen de Recherche et d'Enseignement des Géosciences de l'Environnement, UMR 7330 CNRS, Université Aix-Marseille, F-13545 Aix en Provence Cedex 4, France

Edited by Robert E. Dickinson, University of Texas at Austin, Austin, TX, and approved October 24, 2012 (received for review March 1, 2012)

Wildfire activity in North American boreal forests increased during the last decades of the 20th century, partly owing to ongoing human-caused climatic changes. How these changes affect regional fire regimes (annual area burned, seasonality, and number, size, and severity of fires) remains uncertain as data available to explore fire–climate–vegetation interactions have limited temporal depth. Here we present a Holocene reconstruction of fire regime, combining lacustrine charcoal analyses with past drought and fire-season length simulations to elucidate the mechanisms linking long-term fire regime and climatic changes. We decomposed fire regime into fire frequency (*FF*) and biomass burned (*BB*) and recombined these into a new index to assess fire size (*FS*) fluctuations. Results indicated that an earlier termination of the fire season, due to decreasing summer radiative insolation and increasing precipitation over the last 7.0 ky, induced a sharp decrease in *FF* and *BB ca*. 3.0 kyBP toward the present. In contrast, a progressive increase of *FS* was recorded, which is most likely related to a gradual increase in temperatures during the spring fire season. Continuing climatic warming could lead to a change in the fire regime toward larger spring wildfires in eastern boreal North America.

Canada | drought code | global circulation model | paleoclimate

Recent increases in wildfire frequency and biomass burning in boreal regions in response to ongoing climate warming threaten the carbon sink strength of native ecosystems and, by extension, further contribute to global warming (1). Up-to-date model-based fire predictions indicate that these trends will persist in the coming decades as atmospheric greenhouse gas concentrations will attain unprecedented levels by the end of this century (2, 3). However, model-based fire predictions depend on data collected over short periods—usually less than 100 y—that do not cover a wide range of fire–climate interactions and feedback processes arising from changes in vegetation features. This reduces the robustness of fire predictions, which must therefore be supplemented by paleoecological investigations (4). These investigations often integrate several scientific disciplines, datasets, approaches, and methodologies, thereby providing a robust assessment of how recent trends in fire activity fit into the long-term perspective.

Until now, paleofire reconstructions based on charcoal lacustrine deposits have mostly focused on describing past fire activity in terms of frequency and biomass burning (5). Here we address an additional aspect of fire history and fire–climate relationships, namely, the change in fire size over periods of substantial climate change. To do this, we use sedimentary charcoal records extracted from nine kettle lakes located in the eastern North American boreal forest and model simulations of past climate. We introduce a new metric, developed from the combination of the fire frequency and biomass burning components, which allows us to assess the mean biomass burned per fire. We report on the relationship between components of this index with respect to fire characteristics such as size, and we explore its relationship to long-term regional drought conditions and fire-season length.

Sediment Core Locations

The nine lakes are located along a 350-km east–west transect southeast of the James Bay area (50°N, 80°W; Fig. S1). The lakes were chosen because of their similar size, maximum depth, and shape (Table S1). These physical similarities and the spatial proximity of sites within a unique ecozone (dense coniferous boreal forest) made it possible to construct regional composite records of fire regime variability over the last 7,000 y (hereafter 7 ky; Fig. S2). After the deglaciation ~8 ky ago (kya) depending on areas, trees and woodlands began to rapidly colonize the area without going through an initial tundra phase (6). *Picea mariana* (Mill.) B.S.P. has been the main conifer species dominating the regional vegetation (*P. mariana*–feathermoss bioclimatic zone) since at least 7.5 kya (7, 8). Recent paleofire reconstructions in the western part of the study zone have identified a gradual reduction in fire frequency over the last 3.0 ky (9) in response to a reduction in the length of the fire season (10). Dendrochronological investigations corroborate this finding, highlighting an increase in the fire cycle since the end of the Little Ice Age (11).

Results and Discussion

Paleofire Regime. Variations in charcoal accumulation rate (CHAR, charcoal load per time unit, e.g., $mm^{-2}{\cdot}cm^{-2}{\cdot}y^{-1}$) provide a continuous record of past local fire activity within the sampling resolution of the sediment record. For this study, we used the pooled CHAR data from the nine kettle lakes to infer past regional biomass burning (*RegBB*; *Materials and Methods*). A comparison of *RegBB* with a published stand-replacing fire history (11), in an area encompassing 15,000 km^2, indicated that *RegBB* tracked well mid- to long-term changes in the annual proportion of area burned in the study zone (Fig. S3). The *RegBB* reconstruction thus appears to be an adequate proxy for inferring past regional losses of forest cover. *RegBB* values showed that there was a significant increase in biomass burning between 6.0 and 4.0 kyBP, followed by relative stability from 4.0 to 2.0 kyBP and a reduction during the last 1.5 ky (Fig. 1*A*).

Author contributions: A.A.A., S.G., and Y.B. designed research; A.A.A., O.B., M.P.G., and C.H. performed research; A.A.A., O.B., M.P.G., C.H., F.T., A.E.G., V.V., A.T., L.B., and A.G. analyzed data; and A.A.A., O.B., M.P.G., and C.H. wrote the paper.

The authors declare no conflict of interest.

This article is a PNAS Direct Submission.

Freely available online through the PNAS open access option.

[1]A.A.A. and O.B. contributed equally to this work.

[2]To whom correspondence should be addressed. E-mail: ali@univ-montp2.fr.

This article contains supporting information online at www.pnas.org/lookup/suppl/doi:10.1073/pnas.1203467109/-/DCSupplemental.

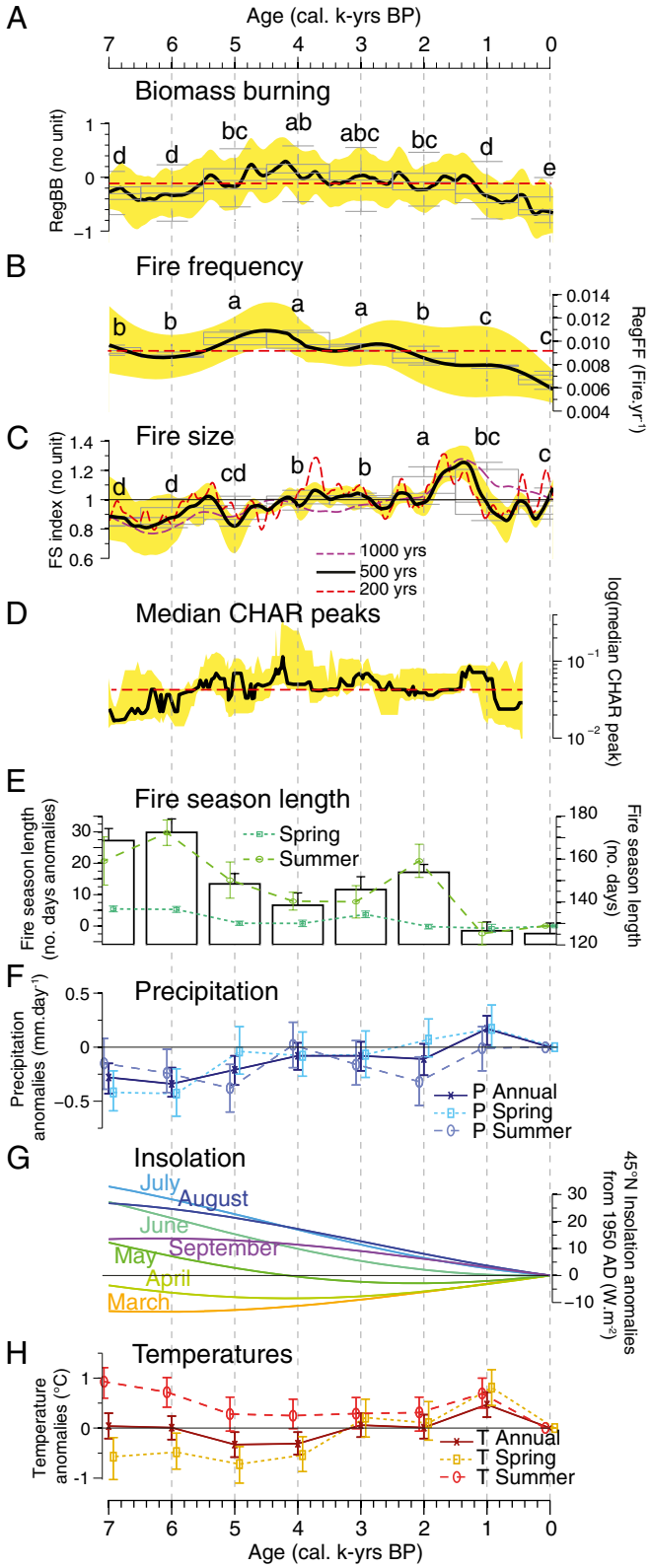

Fig. 1. Reconstructed fire regime history based on the analysis of lacustrine charcoal deposits. (*A*) Biomass burning (*RegBB*) using total charcoal influx. Black line corresponds to the smoothing values using a LOWESS function (500-y time window). The yellow area corresponds to the 90% bootstrap confidence intervals (BCI). The median value for the sequence is represented by the red dashed line. Detected trends were confirmed by box-plot analysis carried out for each 1,000-y period; significance between millennia was assessed using the Wilcoxon rank sum test. A stable amount of biomass that burned from 5.5 to 1.5 kya and a decrease thereafter are recorded. (*B*) Fire frequency (*RegFF*) using the peak components of total charcoal influx, displaying a significant decrease in fire frequency after 3.0 kya. A Gaussian kernel smoothing with a bandwidth of 500 y was used to illustrate the *RegFF* trend. (*C*) Fire size (*FS* index) computed from the ratio *RegBB*/*RegFF* and indicating a significant shift from frequent but small wildfires to infrequent but larger events. The black line represents the median of simulated *FS* index for the 500-y bandwidth; the 200- and 1,000-y bandwidths are represented by the dashed red and purple lines, respectively (*Materials and Methods*). (*D*) Median CHAR peak values ($PEAK_{MED}$) computed across a moving window of 23 fire events (~500-y window; *Materials and Methods*). $PEAK_{MED}$ is herein used as a proxy for fire size. The median value for the sequence is represented by the red dashed line. A gradual increase in $PEAK_{MED}$ was recorded up to 1.5 kya. (*E*) Fire season length assessed on the basis of the number of days with simulated monthly means of daily drought code (DC) values higher than 80 units, showing a decrease in fire-season length over the last 7000 y (spring and summer DCs are indicated by dotted and dashed lines, respectively). Error bars denote the SDs. (*F*) Simulated annual and seasonal precipitation by the UGAMP model (anomalies relative to preindustrial control period (0 kyBP) assumed to be representative of the present-day conditions). (*G*) Monthly radiative insolation at 45°N (35) showing a decrease during the summer months (July to September) and an increase during the spring months (April to June). (*H*) Simulated annual and seasonal air temperatures by the UGAMP model (the same preindustrial period for the present-day reference and anomaly calculation), showing a significant increase in spring temperatures during the last 3.0 ky.

From lacustrine charcoal data it is also possible to deduce the regional fire frequency (*RegFF*) by analyzing peak components of the total CHAR (i.e., significant peak above the background; *Materials and Methods*). As illustrated in Fig. 1*B*, mean *RegFF* underwent a gradual increase between 6.0 and 5.0 kyBP, followed by 3.0 ky of relative stability, with a mean of 0.0097 fire·y^{-1} (90% confidence interval (CI): [0.0080, 0.0120]). This value of *RegFF* corresponds to a mean fire-free interval (MFI) of 103 y [83, 125]. A decrease in *RegFF* occurred between 3.0 and 0 kyBP (Fig. 1*B*). The present-day *RegFF* (0 ky, computed over the last 100 y) is estimated to be 0.0058 fire·y^{-1} [0.0046, 0.0072], i.e., a MFI of 180 y [139, 217]. This MFI is close to the fire cycle estimate derived from the stand-replacing fire history of the study zone (i.e., 171 y with 95% CI [152, 194]) (11).

Usually, fire size and severity (i.e., the loss of tree crown canopy and surface and belowground organic matter during a fire) correspond to metrics related to a given fire event and they may be defined in different ways (12). We consider that fire size and severity are related to the temporal trajectory of mean biomass burned per fire, reflecting part of the loss of organic matter (*RegBB*), modulated by the number of fires through time (*RegFF*). Both severity and size of fires are correlated in eastern boreal North America: Large stand-replacing wildfires (>200 ha) are often severe, with high tree mortality (11, 13). However, below we limit our discussion to fire size on the basis of the observed correlation between *RegBB* and long-term changes in the area burned inferred from fire history studies (14) (*SI Text*). We used the ratio between *RegBB* and *RegFF* to characterize the temporal changes in fire size (Fig. 1*C*; hereafter *FS* index; *Materials and Methods*) at a regional scale:

$$FS = RegBB \Big/ RegFF. \quad [1]$$

Herein, *FS* index values <1 are indicative of a lower mean biomass burned per fire owing to smaller fire sizes, and vice versa. The use of the *FS* index as a proxy for mean fire size is supported by its significant correlation to the changes in the median of the magnitude of CHAR peaks ($PEAK_{MED}$, Fig. 1*D*) from 7.5 ky to present (r = 0.42, 95% bootstrap confidence interval with correction for autocorrelation in data = [0.28, 0.54]). High amplitude of CHAR peak should represent large fire events within the

potential charcoal source area (15). Our interpretation of fire size fluctuations is based on both *FS* index and $PEAK_{MED}$ trends.

Before 4.5 kyBP, *FS* index values were mostly <1 (Fig. 1*C*). The total biomass burned likely resulted mostly from numerous small fires (low $PEAK_{MED}$; Fig. 1*D*). During the period extending between 4.5 kyBP and 2.5 kyBP, *FS* index values were close to 1 and *RegBB* varied in the same range as *RegFF*. The period was likely to be one in which an intermediate fire regime was established, where *RegBB* resulted from small to large fires ($PEAK_{MED}$ mostly varied around the long-term median). This was followed by a gradual increase in the *FS* index until *ca*. 1.5 kyBP. The total biomass burned likely resulted mostly from large fires (high $PEAK_{MED}$; Fig. 1*D*). The last 1.5-ky period was characterized by a decrease in both *RegFF* and *RegBB*: The *FS* index decreased, reaching values close to 1 ($PEAK_{MED}$ was also below the long-term median). Below we provide some potential explanations for the trajectory recorded in fire size, with the climatic hypothesis as the most plausible one.

Climatic Hypothesis. In boreal forests, large-fire years occur as a result of increased late-season burning associated with warm springs followed by dry summers (1, 16). Unsynchronized changes between spring and summer conditions may hence bring unexpected changes in fire metrics like total biomass burned, number of fires, and mean fire size. Such complex effects were tested by analyzing data extracted from the UK Universities Global Atmospheric Modeling Program (UGAMP) (17) general circulation model (GCM) and comparing the modeled regional drought conditions and fire-season length (computed for each 1.0-ky period) with *RegBB*, *RegFF*, and the *FS* index. The fire-season length (Fig. 1*E*) was assessed from the cumulative number of dry days having simulated drought code (DC) (*Materials and Methods*) values above the threshold of 80 units (10). Although a slight increase in simulated fire-season length occurred during the period between 4.0 and 2.0 kyBP, the data confirmed the general multimillennial decreasing trend over the past 7 ky reported by previous studies (10). This long-term modification in simulated fire-season length appears to result from an increase in annual precipitation (Fig. 1*F* and Table 1) along with a decrease in summer radiative insolation (Fig. 1*G* and Table 1).

On the basis of exploratory expressions of the long-term correlations linking fire regime components to climatic variability and orbital forcing (Table 1 and Table S2 and S3), a conceptual scheme can be suggested (Fig. 2). In eastern North American boreal forests, changes in Holocene fire regime were driven ultimately by orbital forcing through spring (April to June) and summer (July to September) radiative insolation. The gradual increase in precipitation, coupled with a decrease in summer insolation, had a negative impact on *RegFF* and *RegBB*, likely from less-efficient ignition. The *FS* index was positively driven by spring climatic conditions, notably through insolation-driven increases in temperature early in the fire season (Table 1). Such evidence for a temperature influence on the size of early-season fires is to our knowledge lacking. To examine whether this effect was plausible, we collected data on sizes of lightning-caused fires in *P. mariana*–feathermoss forests recorded from 1973 to 2009 and analyzed their correlation to monthly mean land temperatures (*SI Text*). Results from this analysis show that the mean fire size in the early-fire season is indeed highly correlated to June temperature: A tripling of the mean fire size occurs with each 1 °C increment (Fig. 3). This result is consistent with data from western United States forests and *P. mariana* forests in Alaska, where it is reported that large (or severe) fire years occur as a result of dry fuel conditions and greater fuel availability occurring with earlier seasonal ice thaw (1, 18). Thus, insolation-driven increases in temperature early in the fire season could have contributed to increasing mean fire size over the past 7 ky in our study zone. The shift in *FS* index has occurred despite the increase in spring and annual precipitation during the Late Holocene, which would have been insufficient to compensate for the effect of spring warming. Intraseasonal variations in rain events distribution may also explain the low impact of precipitation during the spring fire season.

Vegetation Pattern Hypothesis. Ecological processes may be held responsible for the changes observed in the *FS* index. A decrease in fire frequency during the Late Holocene (after 4.0-ky BP) could have favored fuel-load continuity and accumulation (19–21), enhancing the occurrence of large stand-replacing wildfires (22). However, the realism of this vegetation feedback on fire size is questionable when confronted with the existing literature on the subject. Indeed, it is generally accepted in the boreal coniferous forest that the probability of burning is independent of stand age and fuel load after canopy closure at 15 or 20 y (23). Alternatively, changes in vegetation composition toward more fire-prone fuel types could have contributed to the increase in fire size during the Late Holocene (24). Still, pollen records from the study zone suggest that forest composition has remained in a stable state, with woodlands dominated by *P. mariana* since at least 7.5 kyBP (e.g., ref. 8). Nevertheless, slight changes in species abundance, including that of fire-prone species *P. mariana* and *Pinus banksiana* Lamb. (25), could have played a role in the fire size fluctuations recorded by the *FS* index. This long-term feedback of landscape vegetation on wildfire size dynamics must be formally tested by further paleovegetation reconstructions that could infer and quantify past vegetation structuring.

Table 1. Pearson's correlation coefficients between reconstructed fire regime history and main climatic variables

Variables	Fire season length	Spring temperatures	Spring precipitation	Annual precipitation	March insolation	Summer insolation (July, August, September)	*RegBB*	*RegFF*	*FS* index
Fire season length	1								
Spring temperatures	−0.576	1							
Spring precipitation	**−0.832****	**0.670****	1						
Annual precipitation	**−0.913*****	**0.827****	**0.865*****	1					
March insolation	**−0.794****	**0.781****	**0.740****	**0.836*****	1				
Summer insolation	**0.823****	**−0.792****	**−0.816****	**−0.865*****	**−0.976******	1			
RegBB	0.104	−0.237	0.167	−0.096	−0.472	0.316	1		
RegFF	0.432	−0.576	−0.267	−0.475	**−0.827****	**0.723***	**0.857****	1	
FS index	**−0.809****	**0.753****	**0.895*****	**0.856*****	**0.860******	**−0.927******	0.021	−0.475	1

April to June for spring and July to September for summer. Significant correlation coefficients are in boldface type with *P* values reported as follows: *$P < 0.1$; **$P < 0.05$; ***$P < 0.01$; ****$P < 0.001$. Significance was determined using permutation tests with correction for multiple comparisons (*SI Text*). Sample size is $n = 8$ millennia.

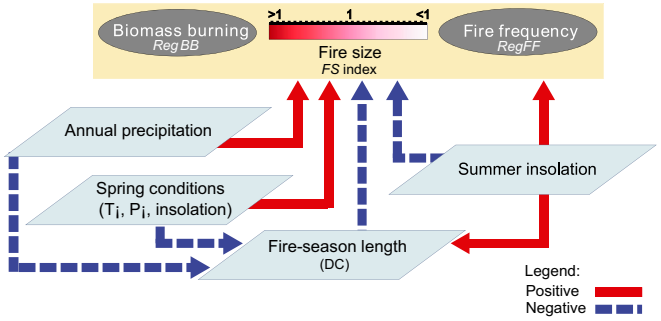

Fig. 2. Conceptual scheme of the balance (ratio) between biomass burned (*RegBB*) and fire frequency (*RegFF*), defining fire size and their relationships to climate conditions and orbital forcing. We deliberately oriented relations of cause and effect, using arrows from the relationships established using the correlation coefficients presented in Table 1. Signs (colors) refer to significant positive or negative correlations, respectively. During the Holocene, the *FS* index has moved along the scale from values <1 to values >1 (Fig. 1*C*) and it stopped twice around a value of 1, owing to different conditions.

Conclusion

Our work suggests that the wet climate that characterized the northeastern American boreal forest during the late Holocene (after 3.0 kyBP) was associated with infrequent wildfires, but these were large in extent. The drier climate that characterized the mid-Holocene (before 3.0 kyBP) was associated with a high fire frequency, but fires were smaller than during the Late Holocene. Fire frequency and total biomass burning were controlled by summer radiative insolation and annual precipitation, whereas fire size was dependent upon spring temperatures and perhaps also abundance of fire-prone species (*P. mariana* and *P. banksiana*) at the landscape level. Climatic conditions during the spring fire season and the precipitation regime will play a key role in future fire risk. Human-caused global warming will probably lead, as summer insolation did in the past, to drier conditions coupled with an increase in the length of the fire season (26). This may increase fire frequency and area burned. However, our results suggest that larger spring wildfires may also be foreseen with climatic warming. An important question is whether signs of such a change in fire regime are currently observable in North America, given the pronounced upward trend in area burned by wildfires observed during the 20th century.

Materials and Methods

RegBB. Total lacustrine charcoal influxes (CHAR, $mm^2 \cdot cm^{-2} \cdot y^{-1}$) are commonly used to decipher past biomass combustion at the regional to continental scale (e.g., refs. 27, 28). Here, the composite record of regional biomass burning was constructed by pooling *Z*-score–transformed individual CHAR series (27) (*SI Text*). This method allowed us to minimize the bias related to taphonomic processes and the changes in sedimentation rates (*SI Text*).

RegFF. The CHAR peak component of the total charcoal influx, corresponding to the high-amplitude signals of the charcoal series, was used to reconstruct local fire events (*SI Text*). The CHAR peak component of the total CHAR series is commonly used to infer local fire frequency, i.e., less than 1.3–3.0 km from the lakeshore (29). Each CHAR peak exceeding the threshold is hereafter assumed to be a fire episode, which represents one or more fires occurring within the charcoal source area and within the median sampling resolution of each sequence. A kernel density smoothing function was used to determine a temporally smoothed fire frequency (*FF*) for each core, on the basis of individual reconstructed fire events (30), and the mean *RegFF* was determined on the basis of pooled *FF* for all lakes (Fig. S4 and *SI Text*).

Fire Size Assessment (*FS* Index). We reconstructed the *FS* index through time, using the formulation bellow:

$$\overline{FS} = \sum_{i=1}^{1,000} \frac{RegBB_i + \beta}{RegFF_i + \beta} \Big/ N.$$

$RegBB_i$ represents 1,000 *RegBB* reconstructions obtained by random resampling of the individual CHAR series, $RegFF_i$ represents 1,000 *RegFF* reconstructions obtained by random resampling of the local *FF* series, *N* is the number of resamplings ($n = 1{,}000$), and β is a constant equal to 1. In order to illustrate high to low frequency trends in the *FS* index, this procedure was reiterated three times using bandwidths equal to 200, 500, and 1,000 y. The 90% confidence intervals are calculated from the true distribution of the 1,000 resampled *FS* index series and are presented for the 500-y bandwidth only. The *FS* index must be considered in evaluating the long-term (centennial to millennial timescale) trajectory of mean size of fire events at the regional scale and not in characterizing the size of individual fires. Also, one should be cautious about the interpretation of potential correlation between *FS* index and *RegFF*, as these are linked by definition and therefore a negative correlation can be expected.

Magnitude of CHAR Peaks. The magnitude of CHAR peaks can be used as a proxy for fire size and severity (15, 31). Hence, we computed the median of the magnitude of detected CHAR peaks, using a running window of 23 CHAR peak samples from 7.5 kya to the present. The use of 23 CHAR peak samples is equal to a window width of ~500 y. For each window, the median was computed 1,000 times, using a bootstrapping method, and a 90% confidence interval was constructed.

Fire Season Length. We used paleoclimatic simulations provided by the UGAMP (17) to develop a mechanistic understanding of the climatic variations associated

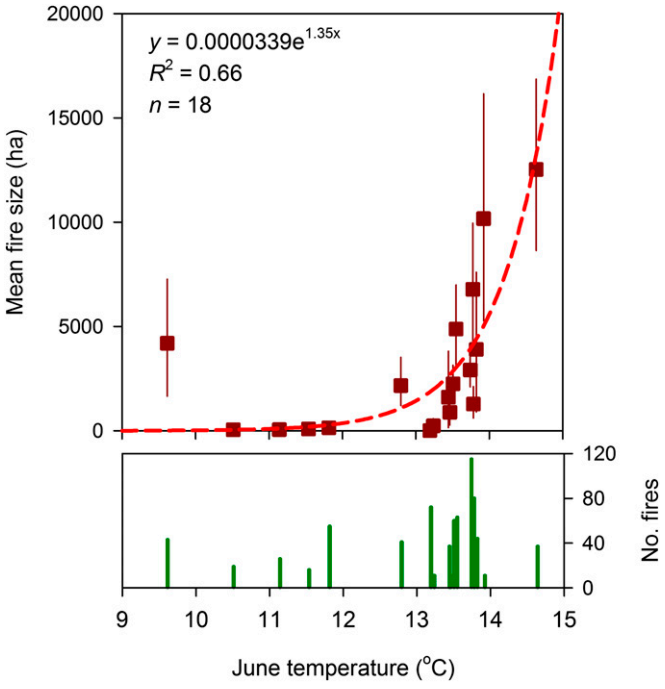

Fig. 3. The effect of mean temperature on mean fire size during early-season burning in *P. mariana*–feathermoss forests of eastern boreal North America. Fire data were those of the Ministère des Ressources Naturelles et de la Faune du Québec. The period of analysis is from 1973 to 2009. Mean fire size was computed for 18 early seasons (April to June), using a minimum threshold of $n = 10$ fires y^{-1}; those seasons in which the number of fires was below this threshold were excluded from analysis. Ignition of 95% of the sampled fires took place after May 27th ($n = 740$ fires in total; *Lower*, sample distributions; correlation between *n* and mean fire size is Spearman's $r = 0.232$, $P = 0.347$). Error bars represent 90% confidence intervals for the means obtained by bootstrap resampling of the fire samples. The dashed line represents the exponential regression of mean fire size on mean temperature. Temperature data (land only) were those of Climate Research Unit TS 3.1 (32), averaged over the domain encompassing 79.5°W–70.0°W and 48.5°N–52.5°N.

with the reconstructed paleofire regime (*SI Text*). A downscaling method was conducted by applying the UGAMP anomalies of temperature and precipitation to the Climate Research Unit climatology dataset Times Series (TS) 2.1 (32). Richardson's (33) weather generator was applied to the simulated time series of monthly temperature and precipitation to derive daily values necessary to compute the DC index of the Canadian Forest Fire Weather Index System (34). A DC value of zero is indicative of saturation and values higher than 400 are indicative of potential deep burning of subsurface heavy fuels.

ACKNOWLEDGMENTS. Financial support was provided by the programs Paléo-environnements, Paléoclimats [Institut Ecologie et Environnement Centre National de la Recherche Scientifique, France] (A.A.A.), the Natural Sciences and Engineering Research Council of Canada (Y.B. and A.A.A.), the Fonds de Recherche Nature et Technologie du Québec (Y.B. and S.G.), the Forest Complexity Modelling program (Natural Sciences and Engineering Research Council, Canada) (O.B.), and the Canadian Forest Service. The research was carried out within the framework of the International Associated Laboratory (France–Canada).

1. Turetsky MR, et al. (2011) Recent acceleration of biomass burning and carbon losses in Alaskan forests and peatlands. *Nat Geosci* 4(1):27–31.
2. Flannigan M, Logan K, Amiro B, Skinner W, Stocks B (2005) Future area burned in Canada. *Clim Change* 72(1):1–16.
3. Soja AJ, et al. (2007) Climate-induced boreal forest change: Predictions versus current observations. *Global Planet Change* 56(3–4):274–296.
4. Whitlock C, Higuera PE, McWethy DB, Briles CE (2010) Paleoecological perspectives on fire ecology: Revisiting the fire-regime concept. *Open Ecol J* 3:6–23.
5. Marlon JR, et al. (2012) Long-term perspective on wildfires in the western USA. *Proc Natl Acad Sci USA* 109(9):E535–E543.
6. Richard PJH (1995) Le couvert végétal du Québec-Labrador il y a 6000 ans BP: Essai [The vegetational cover of Québec-Labrador at 6000 years BP: an essay]. *Géographie Physique et Quaternaire* 49:117–140. French.
7. Garralla S, Gajewski K (1992) Holocene vegetation history of the boreal forest near Chibougamau, central Quebec. *Can J Bot* 70(7):1364–1368.
8. Carcaillet C, et al. (2001) Change of fire frequency in the eastern Canadian boreal forests during the Holocene: Does vegetation composition or climate trigger the fire regime? *J Ecol* 89(6):930–946.
9. Ali AA, Carcaillet C, Bergeron Y (2009) Long-term fire frequency variability in the eastern Canadian boreal forest: The influences of climate vs. local factors. *Glob Change Biol* 15:1230–1241.
10. Hély C, et al. (2010) Eastern boreal North American wildfire risk of the past 7000 years: A model-data comparison. *Geophys Res Lett* 37:L14709 (lett).
11. Bergeron Y, Gauthier S, Flannigan M, Kafka V (2004) Fire regimes at the transition between mixedwood and coniferous boreal forest in northwestern Quebec. *Ecology* 85(7):1916–1932.
12. Keeley JE (2009) Fire intensity, fire severity and burn severity: A brief review and suggested usage. *Int J Wildland Fire* 18(1):116–126.
13. Madoui A, Leduc A, Gauthier S, Bergeron Y (2011) Spatial pattern analyses of post-fire residual stands in the black spruce boreal forest of western Quebec. *Int J Wildland Fire* 19(8):1110–1126.
14. Higuera PE, Whitlock C, Gage JA (2011) Linking tree-ring and sediment-charcoal records to reconstruct fire occurrence and area burned in subalpine forests of Yellowstone National Park, USA. *Holocene* 21(2):327–341.
15. Higuera PE, Sprugel DG, Brubaker LB (2005) Reconstructing fire regimes with charcoal from small-hollow sediments: A calibration with tree-ring records of fire. *Holocene* 15 (2):238–251.
16. Balshi MS, et al. (2009) Assessing the response of area burned to changing climate in western boreal North America using a Multivariate Adaptive Regression Splines (MARS) approach. *Glob Change Biol* 15(3):578–600.
17. Hall MJ, Valdes PJ (1997) A GCM simulation of the climate 6000 years ago. *J Clim* 10 (1):3–17.
18. Westerling AL, Hidalgo HG, Cayan DR, Swetnam TW (2006) Warming and earlier spring increase western U.S. forest wildfire activity. *Science* 313(5789):940–943.
19. Whelan RJ (1995) *The Ecology of Fire* (Cambridge Univ Press, Cambridge, UK).
20. Harper KA, Bergeron Y, Drapeau P, Gauthier S, De Grandpré L (2005) Structural development following fire in black spruce boreal forest. *For Ecol Manage* 206(1):293–306.
21. Brassard BW, Chen HYH, Wang JR, Duinker PN (2008) Effects of time since stand-replacing fire and overstory composition on live-tree structural diversity in the boreal forest of central Canada. *Can J For Res* 38(1):52–62.
22. Westerling AL, Swetnam TW (2003) Interannual to decadal drought and wildfire in the western United States. *Eos Trans AGU* 84(49):545.
23. Macias Fauria M, Johnson EA (2008) Climate and wildfires in the North American boreal forest. *Philos Trans R Soc Lond B Biol Sci* 363(1501):2317–2329.
24. Higuera PE, et al. (2008) Frequent fires in ancient shrub tundra: Implications of paleorecords for arctic environmental change. *PLoS ONE* 3(3):e0001744.
25. Carcaillet C, Richard PJH, Bergeron Y, Fréchette B, Ali AA (2010) Resilience of the boreal forest in response to Holocene fire-frequency changes assessed by pollen diversity and population dynamics. *Int J Wildland Fire* 19(8):1026–1039.
26. Wotton B, Flannigan M (1993) Length of the fire season in a changing climate. *For Chron* 69(2):187–192.
27. Power MJ, et al. (2008) Changes in fire regimes since the Last Glacial Maximum: an assessment based on a global synthesis and analysis of charcoal data. *Clim Dyn* 30(7): 887–907.
28. Clark JS, Royall PD (1996) Local and regional sediment charcoal evidence for fire regimes in presettlement north-eastern North America. *J Ecol* 84(3):365–382.
29. Higuera PE, Gavin DG, Bartlein PJ, Hallett DJ (2010) Peak detection in sediment–charcoal records: Impacts of alternative data analysis methods on fire-history interpretations. *Int J Wildland Fire* 19(8):996–1014.
30. Blarquez O, Carcaillet C, Elzein TM, Roiron P (2012) Needle accumulation rate model-based reconstruction of palaeo-tree biomass in the western subalpine Alps. *Holocene* 22(5):579–587.
31. Colombaroli D, Gavin DG (2010) Highly episodic fire and erosion regime over the past 2,000 y in the Siskiyou Mountains, Oregon. *Proc Natl Acad Sci USA* 107(44): 18909–18914.
32. Mitchell TD, Jones PD (2005) An improved method of constructing a database of monthly climate observations and associated high-resolution grids. *Int J Climatol* 25: 693–712.
33. Richardson CW (1981) Stochastic simulation of daily precipitation, temperature, and solar radiation. *Water Resour Res* 17(1):182–190.
34. van Wagner CE (1987) *Development and Structure of the Canadian Forest Fire Weather Index System* (Canadian Forestry Service, Ottawa).
35. Berger A, Loutre MF (1991) Insolation values for the climate of the last 10 million years. *Quat Sci Rev* 10(4):297–317.